



Effects of Terminal Motif on the Self-Assembly of Dexamethasone Derivatives

Hui Liu, Ailing Yu, Mali Dai, Dan Lin, Deqing Lin, Xu Xu, Xingyi Li* and Yuqin Wang*

School of Ophthalmology & Optometry and Eye Hospital, Institute of Biomedical Engineering, Wenzhou Medical University, Wenzhou, China

OPEN ACCESS

Edited by:

Tianjiao Ji,
Boston Children's Hospital, Harvard
Medical School, United States

Reviewed by:

Jiayan Lang,
Cornell University, United States
Wenshu Zheng,
Tulane University, United States

*Correspondence:

Xingyi Li
lixingyi_1984@163.com
Yuqin Wang
yqwang57@163.com

Specialty section:

This article was submitted to
Supramolecular Chemistry,
a section of the journal
Frontiers in Chemistry

Received: 28 November 2019

Accepted: 07 January 2020

Published: 20 February 2020

Citation:

Liu H, Yu A, Dai M, Lin D, Lin D, Xu X,
Li X and Wang Y (2020) Effects of
Terminal Motif on the Self-Assembly of
Dexamethasone Derivatives.
Front. Chem. 8:9.
doi: 10.3389/fchem.2020.00009

Tailoring the terminal motif of molecules including drugs might significantly affect their self-assembly tendency in aqueous solution, thus providing a rational strategy to modulate its macroscopic characteristics of supramolecular assembly. A model drug of dexamethasone (Dex) was esterified by different fatty acids [succinic acid (SA), glutaric acid (GA), and adipic acid (AA)] and aromatic acid [phthalic acid (PA)] to generate a series of Dex derivatives. Aqueous solution of Dex-SA, Dex-GA, and Dex-AA turned into hydrogel spontaneously after a period time of incubation (24, 48, and 72 h, respectively) via the auto-hydrolytic strategy, while aqueous solution of Dex-PA did not result in hydrogelation during 3 days of incubation. Aqueous solutions of Dex-SA, Dex-GA, and Dex-AA underwent apparent hydrolysis ($10.73 \pm 0.64\%$, $15.17 \pm 2.24\%$, and $17.29 \pm 1.39\%$, respectively), while Dex-PA exhibited a minimal hydrolysis ($<1\%$) in a period of 28 days study, as indicated by *in vitro* hydrolytic test. Morphological observation showed that the hydrogel formed by Dex-SA was composed of uniform nanofibers, while hydrogels formed by Dex-GA, and Dex-AA were derived from irregular particles. The mechanical strength of hydrogel formed by Dex-SA was much bigger than that of hydrogels formed by Dex-GA and Dex-AA, as indicated by rheological test. Moreover, the acylation of Dex did not compromise its potent anti-inflammatory activity in a lipopolysaccharide (LPS)-activated RAW 264.7 macrophage.

Keywords: dexamethasone, self-assembly, terminal motif, drug delivery, hydrogel

INTRODUCTION

Self-assembly of nanomaterials from molecular building block is a promising approach to construct new functional materials for various biomedical applications (e.g., drug delivery, tissue engineering; Blanco et al., 2015; Kalepu and Nekkanti, 2015; Adawiyah et al., 2016; Vader et al., 2016; Zylberberg and Matosevic, 2016; Wu et al., 2017b). Self-assembly is primarily dominated by various non-covalent interactions such as electrostatic, hydrophobic, hydrogen bond, and van der Waals interactions (Zhou and Li, 2017; Yang et al., 2018). The biggest challenge in molecular self-assembly is to precisely control the self-assembly process (nucleation and growth of nanostructure; Zhao et al., 2009; Vemula et al., 2013). In the past several decades, a number of strategies including enzyme, pH condition, light, and so on have been proposed to achieve a spatial and temporal controlled self-assembly of nanomaterials (e.g., peptide, lipid; Vemula et al., 2009, 2013; Mao et al., 2012; Li et al., 2013; Lin and Cui, 2015; Ma et al., 2016; Wang et al., 2017b; Wu et al., 2018). Among these strategies, approaches involving hydrolytic or enzymatic reactions have

gained considerable attention, because they offered great opportunities to elaborately tailor the characteristics of assemblies.

One emerging class of self-assembly system is steroidal agents (e.g., bile salts, sodium deoxycholate) that form numerous supramolecular assemblies (e.g., fiber, tube, particle) and have been reported for a long time (Terech et al., 2002, 2009; Svobodová et al., 2012; Zhang et al., 2017). Similarly, steroidal drugs (e.g., dexamethasone, triamcinolone acetonide) have been widely used to construct supramolecular hydrogel owing to their excellent self-assembly capacity (Wu et al., 2017a; Xiong et al., 2018; Zhou et al., 2018). For instance, Samuel I. Stupp and co-workers reported a dexamethasone-peptide amphiphile that was able to self-assemble into nanofibers via ionic cross-linking strategy, acting as a novel drug delivery system to provide prolonged and localized drug delivery at the site of injection (Webber et al., 2012). More recently, we occasionally found that the succinated dexamethasone (Dex-SA) underwent auto-hydrolysis in phosphate buffered saline (PBS, pH 7.4) to generate a transparent hydrogel (Zhang et al., 2018). Notably, gelation time and mechanical strength of Dex-SA supramolecular hydrogel can be readily modulated by the pH condition of medium and incubation temperature, as well as the hydrogelator concentration. However, since these parameters dramatically influence the macroscopic properties of hydrogels, the effect of

terminal motif on the self-assembly behaviors of dexamethasone has not yet been reported. In this study, we investigated the effects of terminal motif on the self-assembly of dexamethasone derivatives, thus providing the basis to precisely modulate macroscopic characteristics in the supramolecular assemblies.

MATERIALS AND METHODS

Materials

Dex and succinic anhydride were purchased from J&K Scientific Ltd (Beijing, China). Glutaric anhydride was purchased from Beijing Bailingwei Technology Co., Ltd. (Beijing, China). Adpic anhydride was purchased from Nanjing Kangmanlin Biology Technology Co., Ltd. (Nanjing, China). Phthalic anhydride was purchased from Adamas-beta Co., Ltd. (Shanghai, China). Mouse TNF- α DuoSet ELISA (DY410-05) and mouse IL-6 DuoSet ELISA (DY406-05) were obtained from R&D SYSTEMS® (Minneapolis, MN, USA). All other used agents were of analytical grade.

Synthesis and Characterization of Dex Derivatives

As reported previously (Zhang et al., 2018), Dex-SA, Dex-GA, Dex-AA, and Dex-PA derivatives were synthesized via an esterification reaction at room temperature. Briefly, Dex,

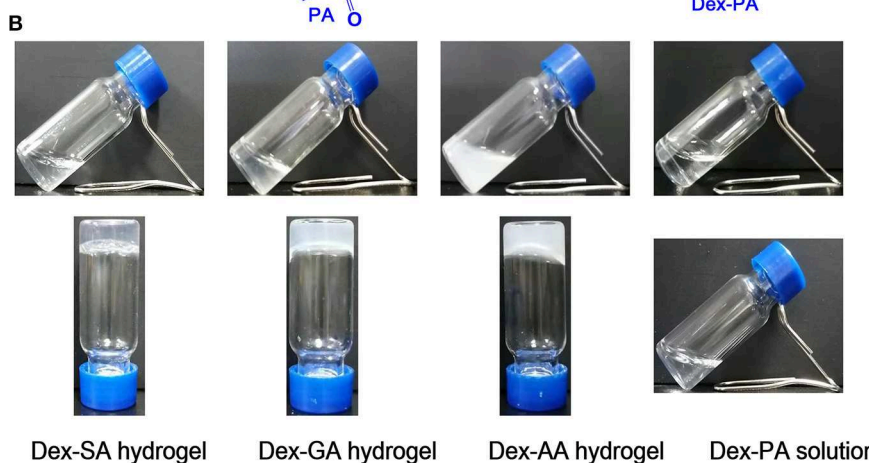
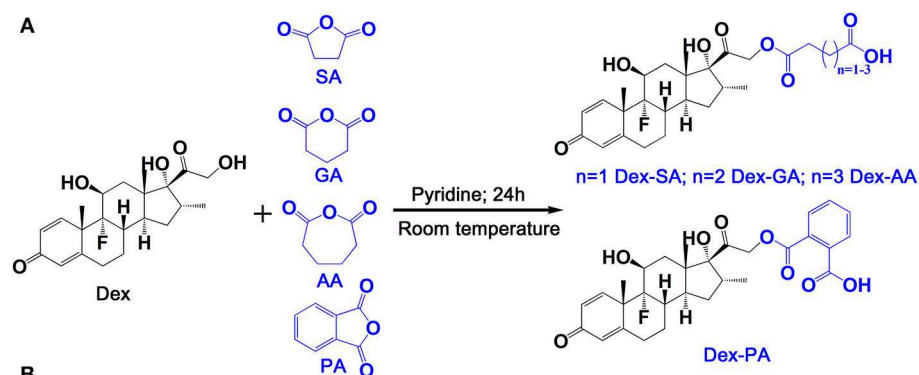


FIGURE 1 | (A) Synthetic scheme of Dex-SA, Dex-GA, Dex-AA, and Dex-PA. **(B)** Appearance of Dex-SA, Dex-GA, and Dex-AA hydrogels and Dex-PA aqueous solution; Dex-SA, Dex-GA, and Dex-AA hydrogels formed at 24, 48, and 72 h with a final concentration at 2 wt%.

and anhydrides with molar ratio at 1:3 were co-dissolved into pyridine for reaction at room temperature overnight. After that, the pyridine was evaporated using a rotary evaporator, and the resulting residues were recrystallized in petroleum ether to afford a series of Dex derivatives. Finally, the obtained products were further confirmed by LC-MS and $^1\text{H-NMR}$ (Figures S1–S8).

Self-Assembly of Dex Derivatives

An indicated amount of Dex derivatives (Dex-SA, Dex-GA, Dex-AA, and Dex-PA) were suspended in PBS (pH 7.4), followed by the addition of a Na_2CO_3 solution (1 equiv to Dex derivatives) to afford a transparent solution at a final concentration of 2 wt%. Sol-gel transition was monitored by an inverted test tube method as reported previously (Joo et al., 2007).

In vitro Hydrolytic Study

The hydrolytic ratio of Dex-SA, Dex-GA, and Dex-AA supramolecular hydrogels and Dex-PA aqueous solution as a function with time was measured by the quantification of the hydrolytic product Dex using HPLC assay. Briefly, 1 ml of Dex-SA, Dex-GA, Dex-AA, and Dex-PA aqueous solution was stored at room temperature for a period of 28 days of study. At predetermined time points, 0.01 ml aliquot of samples were collected and the hydrolytic product Dex was quantified by high-performance liquid chromatography (HPLC, Agilent 1290) with a reversed-phase C18 column (ZORBAX Eclipse XDB-C18, 150×4.6 mm i.d., $5 \mu\text{m}$, Agilent). The mobile phase for the detection of Dex-SA, Dex-GA, and Dex-AA was composed of methanol and 0.1% acetic acid (60/40; v/v), while the mobile phase for the measurement of Dex-PA was composed of methanol and 0.1% acetic acid (70/30; v/v) at a flow rate of 1 ml/min. Aliquots of $20 \mu\text{l}$ of tested samples were injected for HPLC analysis. Detection was performed by a diode array detector (DAD) at 220 nm. The hydrolytic ratio of substrate was calculated using the following equation: Hydrolytic ratio (%) = The amount of Dex at the indicated time point/Total amount of substrate $\times 100$.

Morphology Observation

The morphology of Dex-SA, Dex-GA, and Dex-AA supramolecular hydrogel and Dex-PA aqueous solution was observed by transition electron microscopy (TEM). Samples were pipetted onto a copper grid and stained with a 0.5 wt% phosphotungstic acid solution for TEM observation.

Rheology Test

The rheological properties of Dex-SA, Dex-GA, and Dex-AA supramolecular hydrogels were measured using a TA-AR 2000 rheometer (New Castle, DE, USA). A 40-mm cone plate was used for the experiment. A 0.4 ml hydrogel sample was loaded and a frequency sweep from 0.1 to 100 rad/s was performed.

In vitro Anti-inflammatory Efficacy

To assess the *in vitro* anti-inflammatory efficacy of Dex derivatives (Dex-SA, Dex-GA, Dex-AA, and Dex-PA), we measured the pro-inflammatory cytokine levels in the culture medium using LPS-activated RAW264.7 macrophages. Briefly, RAW264.7 macrophages were seeded at a density of 0.7×10^4

cells per well in a 24-well plate and pre-treated by $10 \mu\text{M}$ Dex, Dex-SA, Dex-GA, Dex-AA, and Dex-PA aqueous solution for 2 h, followed by the challenge with 1000 ng/ml lipopolysaccharide (LPS) for 24 h. Thereafter, the supernatant from each well was collected, and the pro-inflammatory factors including tumor necrosis factor- α (TNF- α) and interleukin-6 (IL-6) levels were measured using an ELISA kit (Neobioscience, Shenzhen, China). The level of nitrite (NO) was detected by the Griess assay

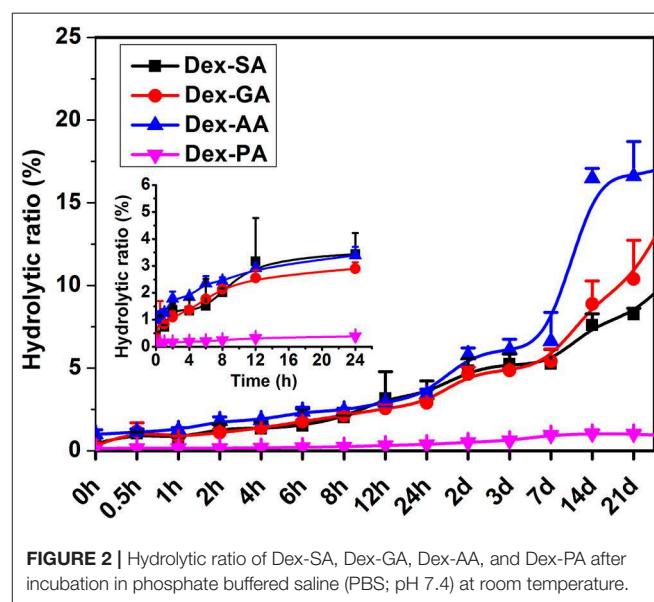


FIGURE 2 | Hydrolytic ratio of Dex-SA, Dex-GA, Dex-AA, and Dex-PA after incubation in phosphate buffered saline (PBS; pH 7.4) at room temperature.

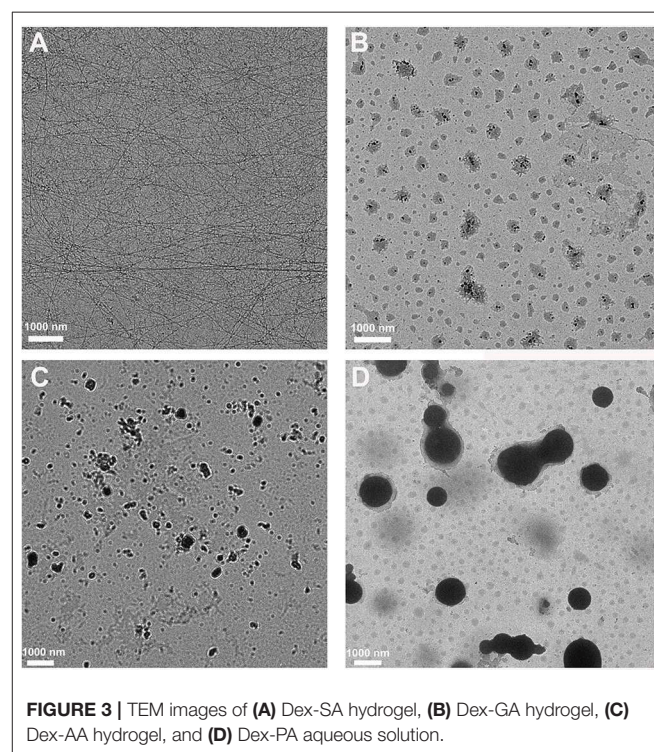


FIGURE 3 | TEM images of (A) Dex-SA hydrogel, (B) Dex-GA hydrogel, (C) Dex-AA hydrogel, and (D) Dex-PA aqueous solution.

as reported previously (Zhou et al., 2018). Cells without any manipulation were used as the negative control.

Statistical Analysis

The values of all experiments were expressed as the mean \pm SD and statistically analyzed by Origin 8.5. *In vitro* anti-inflammatory efficacy data were analyzed by one-way analysis of variance (ANOVA) with Tukey's multiple comparisons test using GraphPad Prism 7.00. Statistical significance was considered at a probability level of $P < 0.05$.

RESULTS AND DISCUSSION

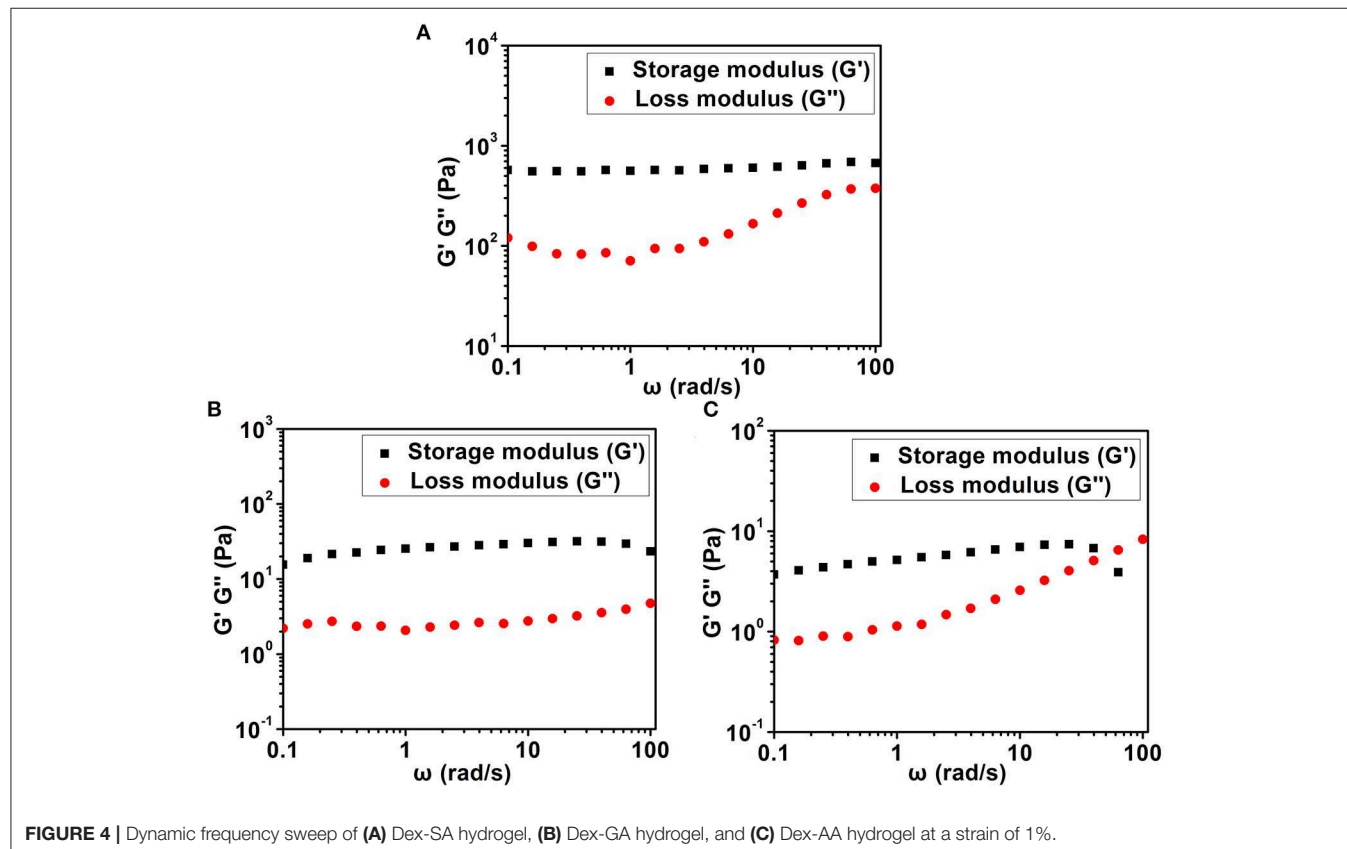
Self-Assembly of Dex Derivatives

Pilot studies have illustrated that the terminal motif of molecules (e.g., drugs, peptide) exhibited a strong influence over the self-assembling capacity of the same self-assembling core (Zhang et al., 2010; Ryan et al., 2011; Wang et al., 2017a). We therefore rationally designed and synthesized four precursors of Dex (Figure 1A; Dex-SA, Dex-GA, Dex-AA, and Dex-PA, respectively). We speculated that the acyl and alkyl chain lengths of the four precursors might dramatically influence the self-assembly tendency of Dex, thus resulting in precisely control macroscopic properties of supramolecular assemblies. We thereafter dissolved the compounds into PBS (pH 7.4) at a final concentration of 2 wt% (20 mg/ml). It is clearly observed that the Dex-SA, Dex-GA, and Dex-PA resulted into a transparent

solution in PBS, while the Dex-AA exhibited a translucent solution (Figure 1B). Aqueous solutions of Dex-SA, Dex-GA, and Dex-AA turned into hydrogels upon incubation at ambient temperature for 24, 48, and 72 h, respectively. The resulting three hydrogels exhibited different appearances. Hydrogel formed by Dex-SA is transparent, and hydrogels formed by Dex-GA and Dex-AA are turbid (Figure 1B). Notably, the hydrogels formed by Dex-GA and Dex-AA occurred the precipitation after 7 days of incubation, while the hydrogel formed by Dex-SA was very stable even up to 7 days storage (Data not shown). Interestingly, there were no obvious changes in aqueous solution of Dex-PA during 3 days of incubation at ambient temperature. All these results suggested that the acyl and alkyl chain lengths had a significant effect on the self-assembly behavior of Dex conjugates.

Hydrolytic Study

The hydrolytic ratio of various Dex conjugates (Dex-SA, Dex-GA, Dex-AA, and Dex-PA) was monitored by measuring the hydrolytic product Dex by HPLC assay. As shown in Figure 2, it is clearly observed that Dex-SA, Dex-GA, and Dex-AA underwent similar hydrolytic behavior with about 3% hydrolysis of total substrate after 24 h incubation in PBS (pH 7.4). It seems to suggest that the hydrolytic rate of Dex-SA, Dex-GA, and Dex-AA was very slow in PBS solution and alkyl chain lengths in the range of 4–6 had no effect on the hydrolytic rate of ester bond. By extending incubation to 28 days, the



hydrolytic rate of Dex-SA, Dex-GA, and Dex-AA accelerated significantly and the hydrolytic ratio of Dex-SA, Dex-GA, and Dex-AA achieved $10.73 \pm 0.64\%$, $15.17 \pm 2.24\%$, and $17.29 \pm 1.39\%$, respectively. Interestingly, Dex-PA resulted in a distinct reduction of the hydrolytic rate in PBS, and the hydrolytic ratio of Dex-PA was $<0.5\%$ after 24 h incubation. Even after 28 days of incubation, the hydrolytic ratio of Dex-PA was still $<1\%$, indicating the relatively stable Dex-PA in PBS solution. This result was in accordance with the previous report of aromatic esters that are relatively stable over the fatty acid esters in most cases owing to the steric hindrance of the aromatic group to increase the activation energy of the hydrolysis (Khuwijitjaru et al., 2004).

Morphological Observation

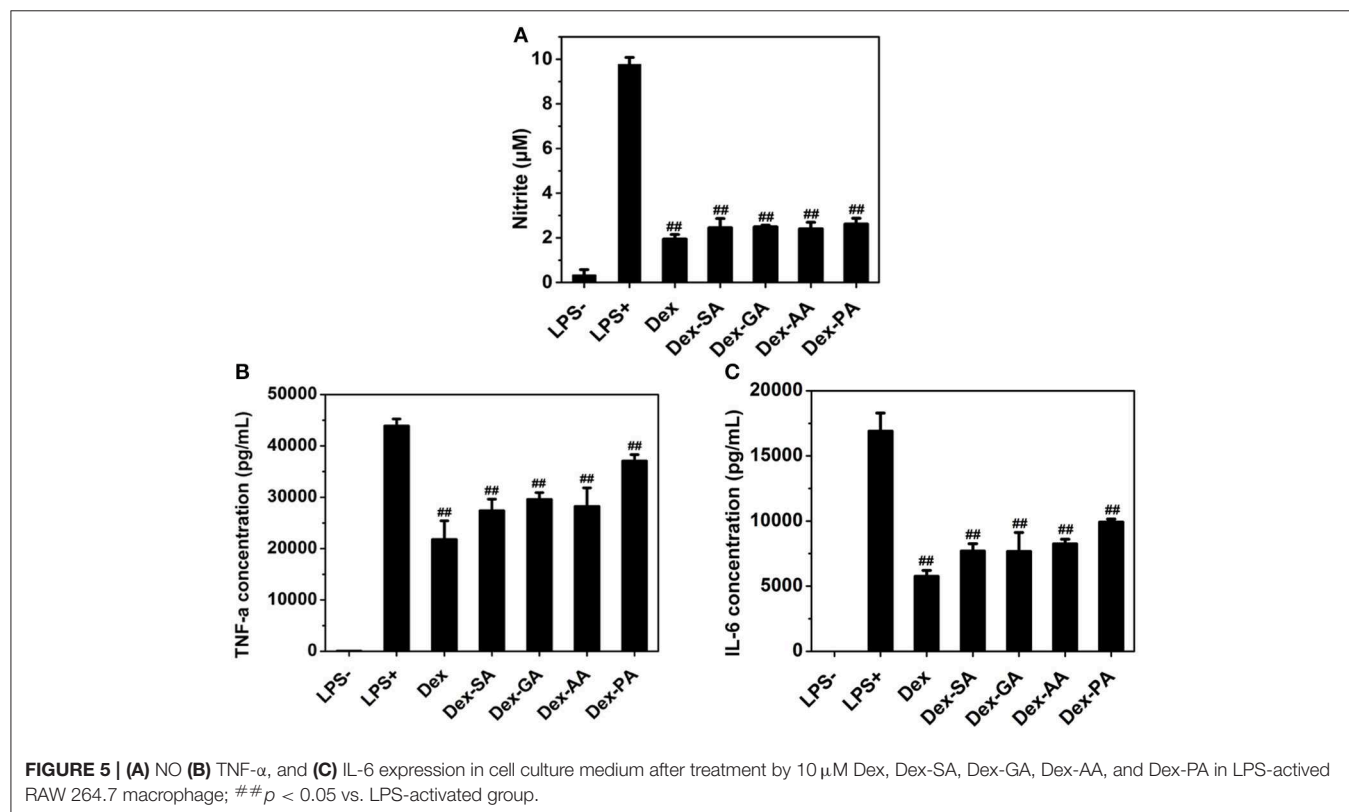
We then adopted transmission electron microscopy (TEM) to visualize the morphology of nanostructures in the resulting hydrogels or solution. As shown in **Figure 3A**, Dex-SA hydrogel displayed the dense and three-dimensional networks of nanofibers. Unlike the Dex-SA hydrogel, Dex-GA, and Dex-AA hydrogels were composed of some irregular particles (**Figures 3B,C**), which tends to aggregate, resulting in the precipitation after 7 days of incubation. It is not surprising that Dex-PA solution was composed of spherical particles ranging 600–1,200 nm in size (**Figure 3D**). These results indicated that the acyl and alkyl chain lengths exert a profound influence on self-assembly propensity and morphology.

Rheology Test

We then used a rheometer to characterize the mechanical properties of various hydrogels. As shown in **Figure 4**, all hydrogels exhibited weak frequency dependence in the range of 0.1–100 rad/s, suggesting the relative elasticity of the hydrogels. More importantly, the storage modulus (G') value of hydrogel formed by Dex-SA was much larger than that of hydrogel formed by Dex-GA and Dex-AA. For instance, the G' value was about 560, 25, and 5 Pa at a frequency of 1 rad/s for hydrogels formed by Dex-SA, Dex-GA, and Dex-AA, respectively. The relatively higher mechanical strength of hydrogel formed by Dex-SA might be ascribed to the formation of nanofibers to support its three-dimensional structure (**Figure 3A**). These results strongly indicated that the mechanical strength of hydrogels were also greatly influenced by the terminal motif of Dex.

In vitro Anti-inflammatory Test

Since macrophage played a very important role in the inflammatory response via the secretion of a variety of factors (Perry et al., 1993; Mantovani et al., 2005; Cohen and Mosser, 2013), such as nitric oxide (NO) and pro-inflammatory cytokines (e.g., IL-1 β , TNF- α , IL-6) after the challenge with an activating stimulus (e.g., lipopolysaccharide), we have investigated the anti-inflammatory activity of various Dex conjugates in an LPS-activated RAW 264.7 macrophage. As presented in **Figure 5**, it was clearly observed that the untreated RAW 264.7 macrophage produced low levels of nitrite (NO), IL-6, and TNF- α in cell culture medium, while the



activated RAW 264.7 macrophage by 1000 ng/ml LPS resulted in the high release of NO, IL-6, and TNF- α to the culture medium. Pretreatment with various Dex conjugates (Dex, Dex-SA, Dex-GA, Dex-AA, and Dex-PA) gave rise to the significant reduction of the NO, IL-6, and TNF- α production to cell culture medium ($^{*}p < 0.05$ vs. LPS-activated group), suggesting that the acylation of Dex did not compromise its potent anti-inflammatory activity.

CONCLUSION

The terminal motif of Dex significantly affects the self-assembly behavior of Dex in aqueous solution. Aqueous solution of Dex-SA, Dex-GA, and Dex-AA turned into hydrogel within 72 h of incubation, and Dex-PA solution kept the clear solution within 7 days of incubation. Dex-SA, Dex-GA, and Dex-AA exhibited a progressive hydrolysis in PBS solution for a period of 28 days study, and Dex-PA did not result in the apparent hydrolysis within 28 days of incubation. Hydrogel formed by Dex-SA was composed of dense and uniform nanofibers, while hydrogels formed by Dex-GA and Dex-AA were made of irregular particles. More importantly, the acylation of Dex did not compromise its potent anti-inflammatory activity in an LPS-activated RAW 264.7 macrophage. Based on these results, we provided the basis to rationally tailor the terminal motif of drugs and thus precisely modulate the self-assembly behavior of Dex conjugates and control the macroscopic characteristics of its supramolecular assemblies without compromising its pharmacological activities.

REFERENCES

- Adawiyah, N., Moniruzzaman, M., Hawatulaila, S., and Goto, M. (2016). Ionic liquids as a potential tool for drug delivery systems. *Medchemcomm* 7, 1881–1897. doi: 10.1039/C6MD00358C
- Blanco, E., Shen, H., and Ferrari, M. (2015). Principles of nanoparticle design for overcoming biological barriers to drug delivery. *Nat. Biotechnol.* 33, 941–951. doi: 10.1038/nbt.3330
- Cohen, H. B., and Mosser, D. M. (2013). Extrinsic and intrinsic control of macrophage inflammatory responses. *J. Leukocyte. Biol.* 94, 913–919. doi: 10.1189/jlb.0413236
- Joo, M. K., Sohn, Y. S., and Jeong, B. (2007). Stereoisomeric effect on reverse thermal gelation of poly (ethylene glycol)/poly (lactide) multiblock copolymer. *Macromolecules* 40, 5111–5115. doi: 10.1021/ma070008u
- Kalepu, S., and Nekkanti, V. (2015). Insoluble drug delivery strategies: review of recent advances and business prospects. *Acta Pharm. Sin. B* 5, 442–453. doi: 10.1016/j.apsb.2015.07.003
- Khuwijitjaru, P., Fujii, T., Adachi, S., Kimura, Y., and Matsuno, R. (2004). Kinetics on the hydrolysis of fatty acid esters in subcritical water. *Chem. Eng. J.* 99, 1–4. doi: 10.1016/j.cej.2003.08.002
- Li, J., Li, X., Kuang, Y., Gao, Y., Du, X., Shi, J., et al. (2013). Self-delivery multifunctional anti-hiv hydrogels for sustained release. *Adv. Healthc. Mater.* 2, 1586–1590. doi: 10.1002/adhm.201300041
- Lin, R., and Cui, H. (2015). Supramolecular nanostructures as drug carriers. *Curr. Opin. Chem. Eng.* 7, 75–83. doi: 10.1016/j.coche.2014.11.005
- Ma, W., Cheetham, A. G., and Cui, H. (2016). Building nanostructures with drugs. *Nano Today* 11, 13–30. doi: 10.1016/j.nantod.2015.11.003
- Mantovani, A., Sica, A., and Locati, M. (2005). Macrophage polarization comes of age. *Immunity* 23, 344–346. doi: 10.1016/j.immuni.2005.10.001

DATA AVAILABILITY STATEMENT

All datasets generated for this study are included in the article/**Supplementary Material**.

AUTHOR CONTRIBUTIONS

XL and YW contributed to the conception and design of the study. HL performed the study and organized the database. XX performed the statistical analysis. HL and AY wrote the first draft of the manuscript. MD, DaL, and DeL wrote sections of the manuscript. All authors contributed to manuscript revision, and read and approved the submitted version.

FUNDING

This research was supported by the Zhejiang Provincial Natural Science Foundation of China (Grant No. LR18H300002), the National Natural Science Foundation of China (Grant No. 31671022, 81971732), the Zhejiang Medicines Health Science and Technology Program (Grant No. WKJ-ZJ-1529), and the Scientific Research Fund of National Health Commission (Grant No. WKJ-ZJ-1707).

SUPPLEMENTARY MATERIAL

The Supplementary Material for this article can be found online at: <https://www.frontiersin.org/articles/10.3389/fchem.2020.00009/full#supplementary-material>

- Mao, L., Wang, H., Tan, M., Ou, L., Kong, D., and Yang, Z. (2012). Conjugation of two complementary anti-cancer drugs confers molecular hydrogels as a co-delivery system. *Chem. Commun.* 48, 395–397. doi: 10.1039/C1CC16250K
- Perry, V. H., Andersson, P. B., and Gordon, S. (1993). Macrophages and inflammation in the central nervous system. *Trends Neurosci.* 16, 268–273. doi: 10.1016/0166-2236(93)90180-T
- Ryan, D. M., Doran, T. M., Anderson, S. B., and Nilsson, B. L. (2011). Effect of C-terminal modification on the self-assembly and hydrogelation of fluorinated Fmoc-Phe derivatives. *Langmuir* 27, 4029–4039. doi: 10.1021/la1048375
- Svobodová, H., Noponen, V., Kolehmainen, E., and Sievänen, E. (2012). Recent advances in steroidal supramolecular gels. *RSC Adv.* 2, 4985–5007. doi: 10.1039/c2ra01343f
- Terech, P., de Geyer, A., Struth, B., and Talmon, Y. (2002). Self-assembled monodisperse steroid nanotubes in water. *Adv. Mater.* 14, 495–498. doi: 10.1002/1521-4095(20020404)14:7<495::AID-ADMA495>3.0.CO;2-9
- Terech, P., Dourdain, S., Bhat, S., and Maitra, U. (2009). Self-assembly of bile steroid analogues: molecules, fibers, and networks. *J. Phys. Chem. B* 113, 8252–8267. doi: 10.1021/jp811217b
- Vader, P., Mol, E. A., Pasterkamp, G., and Schifflers, R. M. (2016). Extracellular vesicles for drug delivery. *Adv. Drug. Deliver. Rev.* 106, 148–156. doi: 10.1016/j.addr.2016.02.006
- Vemula, P. K., Cruikshank, G. A., Karp, J. M., and John, G. (2009). Self-assembled prodrugs: an enzymatically triggered drug-delivery platform. *Biomaterials* 30, 383–393. doi: 10.1016/j.biomaterials.2008.09.045
- Vemula, P. K., Wiradharma, N., Ankrum, J. A., Miranda, O. R., John, G., and Karp, J. M. (2013). Prodrugs as self-assembled hydrogels: a new paradigm for biomaterials. *Curr. Opin. Biotech.* 24, 1174–1182. doi: 10.1016/j.copbio.2013.02.006

- Wang, H., Lu, Z., Wang, L., Guo, T., Wu, J., Wan, J., et al. (2017a). New generation nanomedicines constructed from self-assembling small-molecule prodrugs alleviate cancer drug toxicity. *Cancer Res.* 77, 6963–6974. doi: 10.1158/0008-5472.CAN-17-0984
- Wang, Y., Cheetham, A. G., Angacian, G., Su, H., Xie, L., and Cui, H. (2017b). Peptide-drug conjugates as effective prodrug strategies for targeted delivery. *Adv. Drug Deliv. Rev.* 110–111, 112–126. doi: 10.1016/j.addr.2016.06.015
- Webber, M. J., Matson, J. B., Tamboli, V. K., and Stupp, S. I. (2012). Controlled release of dexamethasone from peptide nanofiber gels to modulate inflammatory response. *Biomaterials* 33, 6823–6832. doi: 10.1016/j.biomaterials.2012.06.003
- Wu, D., Xie, X., Kadi, A. A., and Zhang, Y. (2018). Photosensitive peptide hydrogels as smart materials for applications. *Chinese Chem. Lett.* 29, 1098–1104. doi: 10.1016/j.ccl.2018.04.030
- Wu, W., Zhang, Z., Xiong, T., Zhao, W., Jiang, R., Chen, H., et al. (2017a). Calcium ion coordinated dexamethasone supramolecular hydrogel as therapeutic alternative for control of non-infectious uveitis. *Acta Biomater.* 61, 157–158. doi: 10.1016/j.actbio.2017.05.024
- Wu, X. R., Wu, C. W., Ding, F., Tian, C., Jiang, W., Mao, C. D., et al. (2017b). Binary self-assembly of highly symmetric DNA nanocages via sticky-end engineering. *Chinese Chem. Lett.* 28, 851–856. doi: 10.1016/j.ccl.2017.01.012
- Xiong, T., Li, X., Zhou, Y., Song, Q., Zhang, R., Lei, L., et al. (2018). Glycosylation-enhanced biocompatibility of the supramolecular hydrogel of an anti-inflammatory drug for topical suppression of inflammation. *Acta Biomater.* 73, 275–284. doi: 10.1016/j.actbio.2018.04.019
- Yang, P., Yang, C., Zhang, K., Wang, L., and Wang, H. (2018). KLVFF peptide functionalized nanoparticles capture A β ₄₂ by co-assembly for decreasing cytotoxicity. *Chinese Chem. Lett.* 29, 1811–1814. doi: 10.1016/j.ccl.2018.10.003
- Zhang, M., Fives, C., Waldron, K. C., and Zhu, X. X. (2017). Self-assembly of a bile acid dimer in aqueous solutions: from nanofibers to nematic hydrogels. *Langmuir* 33, 1084–1089. doi: 10.1021/acs.langmuir.6b04033
- Zhang, Y., Kuang, Y., Gao, Y., and Xu, B. (2010). Versatile small-molecule motifs for self-assembly in water and the formation of biofunctional supramolecular hydrogels. *Langmuir* 27, 529–537. doi: 10.1021/la1020324
- Zhang, Z., Yu, J., Zhou, Y., Zhang, R., Song, Q., Lei, L., et al. (2018). Supramolecular nanofibers of dexamethasone derivatives to form hydrogel for topical ocular drug delivery. *Colloids Surf. B Biointerfaces* 164, 436–443. doi: 10.1016/j.colsurfb.2018.01.051
- Zhao, F., Ma, M. L., and Xu, B. (2009). Molecular hydrogels of therapeutic agents. *Chem. Soc. Rev.* 38, 883–891. doi: 10.1039/b806410p
- Zhou, Y., Lei, L., Zhang, Z., Zhang, R., Song, Q., and Li, X. (2018). Cation instructed steroidal prodrug supramolecular hydrogel. *J. Colloid Interface Sci.* 528, 10–17. doi: 10.1016/j.jcis.2018.05.059
- Zhou, Y., and Li, X. (2017). Self-assembled small molecular weight hydrogels of prodrugs. *Chinese Chem. Lett.* 28, 1835–1840. doi: 10.1016/j.ccl.2017.04.033
- Zylberberg, C., and Matosevic, S. (2016). Pharmaceutical liposomal drug delivery: a review of new delivery systems and a look at the regulatory landscape. *Drug Deliv.* 23, 3319–3329. doi: 10.1080/10717544.2016.1177136

Conflict of Interest: The authors declare that the research was conducted in the absence of any commercial or financial relationships that could be construed as a potential conflict of interest.

Copyright © 2020 Liu, Yu, Dai, Lin, Lin, Xu, Li and Wang. This is an open-access article distributed under the terms of the Creative Commons Attribution License (CC BY). The use, distribution or reproduction in other forums is permitted, provided the original author(s) and the copyright owner(s) are credited and that the original publication in this journal is cited, in accordance with accepted academic practice. No use, distribution or reproduction is permitted which does not comply with these terms.